Detection of structural vibration with high-rate GNSS Precise Point Positioning – methodology and case study results

Jacek Paziewski[1], Pawel Wielgosz[2], Rafal Sieradzki[3], Radoslaw Baryla[4]

[1] Institute of Geodesy, University of Warmia and Mazury in Olsztyn, Oczapowskiego 1 st. 10-719 Olsztyn, Poland (jacek.paziewski@uwm.edu.pl)
[2] Institute of Geodesy, University of Warmia and Mazury in Olsztyn, Oczapowskiego 1 st. 10-719 Olsztyn, Poland, (pawel.wielgosz@uwm.edu.pl)
[3] Institute of Geodesy, University of Warmia and Mazury in Olsztyn, Oczapowskiego 1 st. 10-719 Olsztyn, Poland, (rafal.sieradzki@uwm.edu.pl)
[4] Institute of Geodesy, University of Warmia and Mazury in Olsztyn, Oczapowskiego 1 st. 10-719 Olsztyn, Poland, (baryla@uwm.edu.pl)

Key words: *Precise Point Positioning; PPP; GNSS; GPS; structural monitoring, displacements*

ABSTRACT

The core of this contribution is to assess the methodology aiming at the application of un-differenced high-rate GNSS measurements for the characterization of the structural vibration. Since regular Precise Point Positioning (PPP) technique may not meet high-precision requirements of coordinate estimates, a modified processing strategy has been proposed to meet the specific demands of structural displacement monitoring. The algorithms were implemented in the in-house developed GNSS data processing software and were used to assess the case study results. For the purpose of the experimental verification of the methodology we have set up a field experiment taking advantage of an in-house made device which simulated dynamic horizontal displacements of the GNSS antenna. The device has been designed and constructed to ensure a periodic motion with modifiable characteristics. In this experiment we have set up amplitudes from 1.5 up to 9 mm and a single frequency equal to 3.80 Hz. The analysis was performed using 100 Hz multi-GNSS measurements. The results have confirmed the applicability of modified PPP technique for providing reliable and consistent results with the precision of the dynamic displacements at the level of several millimeters.

I. Introduction

A. *General Instructions*

Among the years GNSS technology has proved its usability for seismic and geodynamics studies, surveying, deformation monitoring as well as for dynamic displacement detection including structural monitoring (Psimoulis et al 2008, Avallone et al 2011, Geng et al 2016). The methods used for the characterization of the structural vibration ought to satisfy the highest demands in terms of precision, reliability and high temporal resolution. Hence, in contrary to geodynamic and seismic studies, in structural monitoring it is required to employ observations with as high as possible temporal resolution, even up to 100Hz. Such kind of data allows the assessment of the structure response in the broad spectrum of frequency domain (Yi et al. 2013). The specific goal of such investigations is the characterization of the analyzed structure under different ambient excitations (Yu et al. 2014). Hence it is feasible to evaluate the impact of external forces and conditions taking advantage of real measurements and numerical models of the structures.

Thanks to the development of the hardware (receivers and antennas) and processing algorithms, GNSS technology is now considered as a reliable source of information on health of various structures including bridges, tall buildings etc. (Nickitopoulou et al 2006, Li et al 2006). Among a number of GNSS positioning algorithms, there are a few which can meet the specific demands of structural monitoring. They include a common relative approach based on double-differenced data (RTK) as well as the newer method - precise point positioning (PPP) - performed with undifferenced phase and code measurements (Kouba and Héroux 2001). The former is considered as the most precise method of coordinate estimation. Nevertheless, recent contributions have also confirmed the usability of PPP to such applications. In this case we observe a clear benefit from the application of multi-frequency and multi-constellation signals (El-Mowafy et al. 2016, Paziewski et al 2018a). On the other hand, PPP method requires dedicated processing methodology to address the requirements of sub-centimeter high rate displacements detection.

The goal of this contribution is to present and assess dedicated processing strategy based on Precise Point Positioning method, which is suitable for high-rate and high-precision displacement detection. For the experimental verification of the methodology we have set up a field experiment taking advantage of an in-house made device which artificially triggered dynamic horizontal displacements of the GNSS antenna. The device has been designed to ensure a periodic motion

of antenna with selected amplitude and frequency. In the field experiment we have set up amplitudes from 1.5 up to 9 mm and 3.80 Hz frequency of motion. The tests were conducted using GPS+Galileo+BDS data with 100 Hz sampling rate. At this point it should be noted that the high-rate PPP positioning is not supported by any commercial software. Hence, all computations were performed with in-house developed software with implemented high-rate PPP data processing.

This contribution is organized as follows. In the next section we briefly present the methodology of high-rate PPP. The following sections describe the experiment design and discuss the results. The last section is devoted to conclusions and perspectives.

II. METHODOLOGY

A. *Multi-GNSS PPP observational model*

The starting point of our strategy is well-known geometry-based observational model based on ionosphere-free linear combination (IF-LC) of phase and pseudorange observations. The undifferenced phase and code observations collected with selected frequency (*n*) may be denoted as below:

$$\lambda_n \varphi_{l,n}^i = \rho_l^i + c(t_l - t^i) + \lambda_n\left(b_{l,n} - b_n^i\right) + \alpha_l^i ZTD_l - I_{l,n}^i + \lambda_n M_{l,n}^i + \epsilon_{l,\varphi,n}^i \quad (1)$$

$$P_{l,n}^i = \rho_l^i + c(t_l - t^i) + \left(d_{l,n} - d_n^i\right) + \alpha_l^i ZTD_k + I_{l,n}^i + \epsilon_{l,P,n}^i \quad (2)$$

where:

λ is the wavelength on selected frequency signal,
φ is the phase observable in cycles,
P is the pseudorange in meters,
l and *i* represent station and satellite respectively,
ρ is the geometric range between satellite and station,
t_l and t^i are the receiver and satellite clock corrections in seconds, respectively,
c is the speed of light in meters per second,
b_l and b^idenote the frequency-dependent receiver and satellite phase delays in cycles, which includes initial and hardware phase biases,
d_l and d^i are the frequency-dependent receiver and satellite code biases in meters,
α refers to the troposphere mapping function coefficient,
ZTD denotes the zenith tropospheric delay
I_l^i denotes slant ionospheric delay,
M is the noninteger phase ambiguity which combines integer ambiguity term and initial phase at the receiver and satellite terms,
ϵ denotes the observational noise.

Taking advantage of dual-frequency observations we can form ionosphere-free linear combination (Kouba and Héroux 2001) of phase and pseudorange signals and eliminate first order of ionospheric delay as follows:

$$\Phi_{l,IF}^i = \left(f_1^2 \Phi_{l,1}^i - f_2^2 \Phi_{l,2}^i\right)/(f_1^2 - f_2^2) \quad (3)$$

$$P_{l,IF}^i = \left(f_1^2 P_{l,1}^i - f_2^2 P_{l,2}^i\right)/(f_1^2 - f_2^2) \quad (4)$$

where:

Φ is the phase observable in the units of meters corresponding to particular frequency or its combination,
f_1, f_1 denote two selected frequencies for each constellation (e.g. L1 & L2, E1 & E5a, B1 & B2 in the case of GPS, Galileo and BDS constellations).

Considering multi-constellation observables we are obliged to account for time scale inter system bias. This can be done by choosing one of the GNSS system time scales as the pivot and parametrisation of the inter-constellation time difference. The other possibility is to parametrize receiver clock correction combined with receiver hardware delays individually for each GNSS system. Hence the applied multi-constellation PPP observational model is given as follows (5-10). The equations are derived for multi-constellation (g-GPS, e-Galileo, b-BDS) signals.

$$\Phi_{l,IF}^i = \rho_l^i + c\bar{t}_l^g + \alpha_l^i ZTD_l + B_{l,IF}^i + \epsilon_{l,\varphi,IF}^i \quad (5)$$

$$P_{l,IF}^i = \rho_l^i + c\bar{t}_l^g + \alpha_l^i ZTD_l + \epsilon_{l,P,IF}^i \quad (6)$$

$$\Phi_{l,IF}^j = \rho_l^j + c\bar{t}_l^e + \alpha_l^j ZTD_l + B_{l,IF}^j + \epsilon_{l,\varphi,IF}^j \quad (7)$$

$$P_{l,IF}^j = \rho_l^j + c\bar{t}_l^e + \alpha_l^j ZTD_l + \epsilon_{l,P,IF}^j \quad (8)$$

$$\Phi_{l,IF}^k = \rho_l^k + c\bar{t}_l^b + \alpha_l^k ZTD_k + B_{l,IF}^k + \epsilon_{l,\varphi,IF}^k \quad (9)$$

$$P_{l,IF}^k = \rho_l^k + c\bar{t}_l^b + \alpha_l^k ZTD_k + \epsilon_{l,P,IF}^k \quad (10)$$

where:

i, j, k denote selected satellites of GPS, Galileo and BDS constellations, respectively;
$\{\bar{t}_l^g, \bar{t}_k^e, \bar{t}_k^b\}$ are receiver clock corrections combined with the receiver hardware delays corresponding to selected GNSS constellations,
$\{B_{l,IF}^i, B_{l,IF}^j, B_{l,IF}^k\}$ denote ionosphere-free combined non-integer parameters including carrier-phase ambiguity terms coupled with the satellite and the receiver phase biases.

Since the approximate position of the antenna is known, this can be constrained with appropriate a priori weight in the processing providing faster convergence. The details of the employed PPP processing strategy including correction models are given in Table 1.

Table 1. PPP processing strategy.

Signals	phase and code GPS L1&L2 BDS B1&B2 and Galileo E1&E5a
Observations	Undifferenced ionosphere-free linear combination (IF-LC)
Weighting scheme	Elevation-dependent weighting
Elevation cutoff angle	10°
Sampling rate	0.01 s (100 Hz)
Troposphere delay modelling	Estimation of the residual ZTD, a priori Modified Hopfield model + Global Mapping Function
Ionosphere delay modelling	First order of ionospheric delay eliminated taking advantage of IF-LC
Type of the solution	Float kinematic
Stochastic modelling: A priori standard deviation of observations	0.6 m/ 0.006 m for code/phase of GPS and Galileo signals, respectively; BDS signals downweighted by the value of 20%.
Satellite orbits and clocks	Precise CODE (interval: orbits 5 min; clocks 30 s)
Estimation method	Least squares with a priori parameter constraints

B. *PPP coordinate time series filtration for the extraction of the dynamic displacement*

It is well known that the high accuracy of PPP solution (up 1 cm) can be reached after long (e.g. 24h) static solution (Choy et. al 2017). However, in structural monitoring and displacement detection studies the observational session are commonly much shorter. Moreover, the PPP-derived coordinate time series are the subject of many un-modelled effects or residual biases which may affect the estimated position and cause low frequency coordinate variations. As a result we cannot expect to provide the mm-level position with regular PPP even employing multi-constellation and multi-frequency observations. In order to handle these adverse effects in the coordinate time series and reach the highest possible accuracy of displacements, we propose to employ a filtration of coordinate estimates time series. It allows the extraction of high-frequency pattern corresponding to the dynamic displacement of the GNSS antenna. For this purpose we used high-pass Butterworth filter.

III. Experiment Design and Results

A. *Experiment design*

In the experiment we used a prototype shake table, which is responsible for simulating displacements of the GNSS antenna with high level of stability in terms of frequency and amplitude (Fig.1). This device is capable to set the periodical motion steered by control system in single horizontal direction. The advancement of the proposed solution is the ability to set in motion of two GNSS antennas oscillating with the same amplitude and frequency. It should be highlighted that generally commercial systems allow for single antenna application. With the developed device we are able to simulate the antennas' periodical motion with the frequency up to 25 Hz and dedicated amplitude in a range 1-85 mm ±0.5 mm. Moreover the developed shake table is fully portable, which makes the opportunity to perform field experiment at any place using selected test area and GNSS reference stations.

Figure 1. In-house developed portable shake table system during data collection.

In the experiment we have used GNSS observational data collected by Topcon Net-G5 multi-GNSS receiver with the interval of 100 Hz. Additionally, 4 km distant Trimble NETR9 receiver was used to collect data for 50Hz RTK solution, which served as a benchmark result. Both sites were occupied by geodetic antennas: JAV_GRANT-G3T and TRM59800.00, respectively. During the experiment the receivers tracked GPS (up to 9), Galileo (5) and BDS (2-3) satellites (Figure 2). The entire observational session lasted ~1h and was divided into sub-sessions with different characteristic of the GNSS antenna motion. During first 10 minutes the antenna was static; hence this period was used for initial evaluation of the determined displacements accuracy.

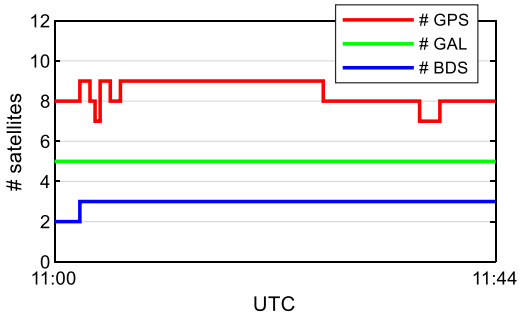

Figure 2. Number of satellites tracked during the experiment.

B. *Evaluation of the accuracy of the high-rate PPP displacements determination*

In the first step we aim to evaluate the accuracy of the small scale coordinate displacements. For this purpose we use a coordinate time series of the period when the GNSS antenna was motionless (first 10 min of the session). Hence any deviation for the reference position can be considered as coordinate error. The coordinate time series were filtrated to retrieve only small scale high-rate coordinate changes (sub-centimeter level).

In the right panel of Fig.3 are given the histograms of the coordinate residuals obtained with GPS+Galileo+BDS (G+E+C) PPP during static period. For the comparison purpose, the left panel presents the corresponding values derived from RTK short baseline solution. The standard deviation (*std*) of the coordinate residuals derived from multi-constellation PPP solution reached the level of 2.7-2.8 mm and 5.3 mm in the case of horizontal and height components, respectively. These statistics are slightly higher than the corresponding values obtained from RTK solution where *std* of N, E components were in the range of 1.8-1.9 mm and U at the level of 3.5 mm. The corresponding result obtained for PPP using only GPS system were very similar to multi-GNSS results (Table 2).

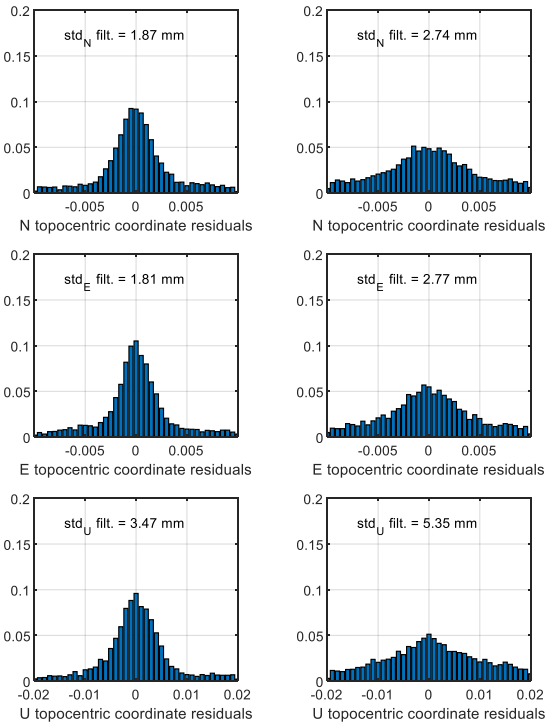

Figure 3. Histograms of coordinate residuals: G+E+C RTK – left panel, G+E+C PPP - right panel.

Table 2. Evaluation of the coordinate time series noise - statistics of coordinate residuals.

	std_N [mm]	std_E [mm]	std_U [mm]
RTK G+E+C	1.9	1.8	3.5
PPP G	2.8	2.8	5.3
PPP G+E+C	2.7	2.8	5.3

Hence, we can conclude that for such application, multi-GNSS signals do not importantly improve the precision of the solution, and the final noise of coordinate time series. As former studies showed multi-GNSS signals, however, contribute to time to fix and final accuracy of the position (Paziewski et al 2018b), which is however of lower importance in this case.

C. *Experiment results and discussion*

The applicability of the modified PPP processing strategy for small-scale dynamic displacements determination was evaluated by the comparison to the benchmark RTK solution and to the true values of the amplitude and frequency of GNSS antenna motion simulated by the shake table system. In order to extract small scale high rate displacements we have employed the high-pass filtering of the coordinate time series. In this experiment we used high-pass Butterworth filter with cut-off period set to 1 s. This way we have handled the low-frequency effects in the PPP coordinate time series, which are mainly caused by residual GNSS positioning errors and not fully converged position.

The horizontal oscillations of the antenna were simulated with the frequency of 3.80 Hz and three different amplitudes equal to 9 mm, 6 mm and 1.5 mm, respectively. Each session with different characteristics of the motion lasted about 5 minutes.

Figure 4 and 5 present samples of the displacement time series derived from multi-GNSS PPP and multi-GNSS RTK solution. The values are given separately for E-W (Fig. 4) and N-S components (Fig. 5). RTK solution was obtained with 50 Hz (due to observation interval of reference station), whereas PPP with 100 Hz.

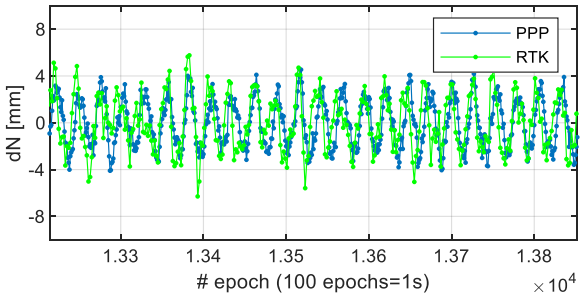

Figure 4. Displacement time series obtained with multi GNSS 50 Hz RTK and 100 Hz PPP. N-S coordinate component.

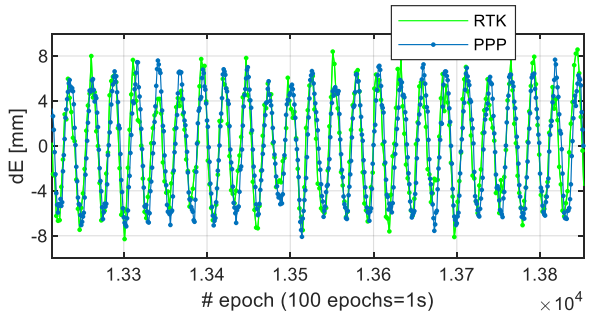

Figure 5. Displacement time series obtained with multi GNSS 50 Hz RTK and 100 Hz PPP. E-W coordinate component.

Tables 3, 4 and 5 provide the frequency responses obtained from Fourier Transformation (FT). In the all cases the FT gave in a result very close values of the motion frequency (3.774 - 3.778 Hz), which are consistent with the designed value of 3.80 Hz. The detected amplitudes of the motion derived from PPP coordinate time series analysis were also close to the values designed in the experiment. The differences between benchmark amplitude of the antenna motion and the mean amplitudes obtained from PPP were lower than 1 mm when simulating 9 mm and 6 mm amplitude motion (Table 3 and 4). Slightly higher discrepancies were obtained in the case of 1.5 amplitude motion (Table 5). In this case the mean amplitudes detected with PPP were in the range of 2.0 – 2.8 mm depending on the processing strategy – GPS or multi GNSS constellation PPP, respectively. We should however note that it is extremely difficult to detect such small displacements with absolute GNSS positioning methods, since we are below the level of observational noise. On the other hand, as it can be clearly seen from Figures 6-7 and Table 5 even in this case we were able to correctly detect the frequency of the motion.

Table 3. Frequency response extracted from N,E displacement time series when simulating antenna oscillation of 9 mm amplitude.

	F_N [Hz]	F_E [Hz]	A [mm]	Benchmark values	
				F [Hz]	A [mm]
RTK G+E+C	3.775	3.775	**9.1**	3.80	**9.0**
PPP G	3.778	3.778	**10.0**		
PPP G+E+C	3.778	3.778	**10.0**		

Table 4. Frequency response extracted from N,E displacement time series when simulating antenna oscillation of 6 mm amplitude.

	F_N [Hz]	F_E [Hz]	A [mm]	Benchmark values	
				F [Hz]	A [mm]
RTK G+E+C	3.777	3.777	**7.6**	3.80	**6.0**
PPP G	3.777	3.777	**6.9**		
PPP G+E+C	3.777	3.777	**6.9**		

Table 5. Frequency response extracted from N,E displacement time series when simulating antenna oscillation of 1.5 mm amplitude.

	F_N [Hz]	F_E [Hz]	A [mm]	Benchmark values	
				F [Hz]	A [mm]
RTK G+E+C	3.773	3.773	**3.1**	3.80	**1.5**
PPP G	3.774	3.774	**2.0**		
PPP G+E+C	3.774	3.774	**2.8**		

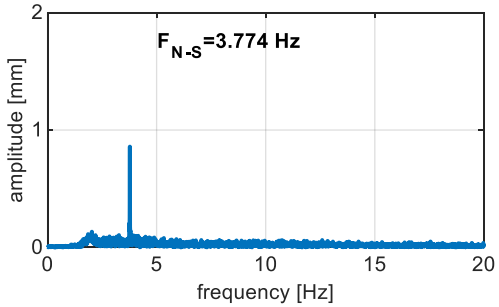

Figure 6. Frequency response at the N-S direction extracted from GPS-PPP displacement time series when simulating antenna oscillation of 1.5 mm amplitude and 3.80 Hz frequency.

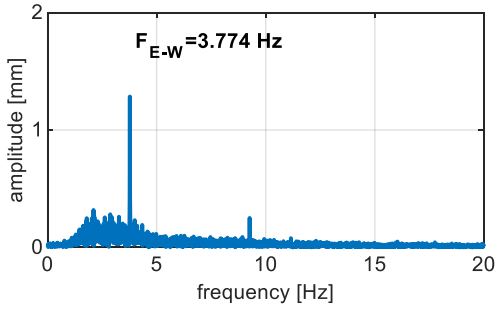

Figure 7. Frequency response at the E-W direction extracted from GPS-PPP displacement time series when simulating antenna oscillation of 1.5 mm amplitude and 3.80 Hz frequency.

IV. Summary

In this paper we have presented the developed processing strategy based on kinematic PPP solution suited for high-rate small scale displacements detection. The method was validated with the field experiment taking advantage of in-house developed shake-table system simulating oscillations of the antenna with the frequency of 3.80 Hz and amplitudes of 9 mm, 6 mm, and 1.5 mm, respectively. The results justified high applicability of the method, since we were able to detect the frequency and amplitude of the simulated dynamic displacements with high level of accuracy. The differences between PPP-derived and true amplitude of the simulated displacements were in the range of 0.5-1.3 mm.

V. Acknowledgements

The work in this contribution was supported by the National Science Centre, Poland: project No. 2016/23/D/ST10/01546.

References

Avallone, A., Marzario, M., Cirella, A., Piatanesi, A., Rovelli, A., Di Alessandro, C., D'Anastasio, E., D'Agostino, N., Giuliani, R., Mattone, M. (2011). Very high rate (10 Hz) GPS seismology for moderatemagnitude earthquakes: the case of the Mw 6.3 L'Aquila (central Italy) event. *Journal of Geophysical Research,* 116:B02305

Choy, S., Bisnath, S., Rizos, C., (2017). Uncovering common misconceptions in GNSS Precise Point Positioning and its future prospect. *GPS Solutions* 21(1):13-22.

El-Mowafy, A., Deo, M., Rizos, C. (2016). On biases in Precise Point Positioning with multi-constellation and multi-frequency GNSS data, *Measurement Science and Technology* 27(3): 035102.

Geng, T., Xie, X., Fang, R., Su, X., Zhao, Q., Liu, G., Li, H., Shi, C., Liu, J. (2016). Real-time capture of seismic waves using high-rate multi-GNSS observations: Application to the 2015 Mw 7.8 Nepal earthquake, *Geophysical Research Letters* 43: 161–167.

Kouba, J., and Héroux, P. (2001). Precise point positioning using IGS orbit and clock products. *GPS Solutions* 5(2):12-28, doi:10.1007/PL00012883.

Li, X., Ge, L., Ambikairajah, E., Rizos, C., Tamura, Y., Yoshida, A. (2006). Full-scale structural monitoring using an integrated GPS and accelerometer system, *GPS Solutions* 10:233-247.

Nickitopoulou, A., Protopsalti, K., Stiros, S., (2006). Monitoring dynamic and quasi-static deformations of large flexible engineering structures with GPS: accuracy, limitations, and promises. *Engineering Structures,* 28:1471–1482.

Paziewski, J., Sieradzki, R., Baryla, R. (2018a). Multi-GNSS high-rate RTK, PPP and novel direct phase observation processing method: application to precise dynamic displacements detection, *Measurement Science and Technology*, 29 035002(15pp).

Paziewski, J., Sieradzki, R., Wielgosz, P. (2018b). On the Applicability of Galileo FOC Satellites with Incorrect Highly Eccentric Orbits: An Evaluation of Instantaneous Medium-Range Positioning. *Remote Sensing* 10(2) 208.

Psimoulis, P.A., Pytharouli, S., Karambalis, D., Stiros, S.C., (2008). Potential of global positioning system (GPS) to measure frequencies of oscillations of engineering structures. *Journal of Sound and Vibration* 318:606–623.

Yi, T.H., Li, H.N., Gu, M. (2013). Experimental assessment of high-rate GPS receivers for deformation monitoring of bridge, *Measurement* 46: 420–432.

Yu, J. Meng, X., Shao, X., Yan, B., Yang, L. (2014). Identification of dynamic displacements and modal frequencies of a medium-span suspension bridge using multimode GNSS processing, *Engineering Structures* 81: 432–443.